EFFECT OF BISMUTH IN LEAD GERMANATE GLASS SYSTEM ON SHIELDING PROPERTIES FOR DEVELOPMENT OF GAMMA-RAYS SHIELDING MATERIALS

M. I. SAYYED[a], M. G. DONG[b], M. H. M. ZAID[c,d], K. A. MATORI[c,d, *], H. A. A. SIDEK[c], V.P. SINGH[e]

[a]*Department of Physics, Faculty of Science, University of Tabuk, Tabuk, Saudi Arabia*

[b]*Department of Resources and Environmental, Northeastern University, Shenyang 110004, China*

[c]*Department of Physics, Faculty of Science, Universiti Putra Malaysia, 43400 UPM Serdang, Selangor, Malaysia*

[d]*Materials Synthesis and Characterization Laboratory, Institute of Advanced Technology, Universiti Putra Malaysia, 43400 UPM Serdang, Selangor, Malaysia*

[e]*Department of Physics, Karnatak University, Dharwad 580003, India*

In this study, the shielding properties of bismuth lead germanate (BPG) glass system in composition $x(Bi_2O_3)40\text{-}x(PbO)60(GeO_2)$ where x = 0 to 40 mol% have been investigated. The shielding parameters, mass attenuation coefficients(μ/ρ), mean free path (MFP) and half value layer (HVL) values have been computed using WinXCom program and variation of shielding parameters of the BPG glasses are discussed for the effect of photon energy and Bi_2O_3 addition into the glasses. The replacement of PbO by Bi_2O_3 causes an increase in mass attenuation coefficient, while the MFP and HVL values were decreased. The investigation would be very useful for shielding applications in nuclear technologies.

(Received February 1, 2017; Accepted January 2, 2018)

Keywords: Bismuth lead germanate glasses; Shielding parameter; Mass attenuation coefficient; WinXCom

1. Introduction

Research interest on germanate glasses has been encouraged by their excellent properties like good thermal stability, chemical durability, mechanical strength and higher solubility of rare earth ions [1-3]. Germanate glasses also have potential applications in for optical lasers and fiber optical amplifiers because of the advantages of low phonon energy and good infrared transmission in a wide wavelength range compared with other oxide glass [4-6]. Thus, from the viewpoint of technological application, germanate glasses are provides the potentially to developed a more efficient medium for shielding materials. Besides, germanate glasses are a suitable material for shielding due to their large transmittance window (from visible to the infrared region) and a low phonon energy (800 cm^{-1}) when compared with silicate glasses (1150 cm^{-1}) [7]. Other properties of the germanate glasses are its high refractive index (~2) and a large chemical stability [8].

The lead oxide (PbO) is known as a non-conventional glass former, since it can act as a glass former or as a modifier [9-11]. The role is determined by its concentration and by the type of bond between lead and oxygen. Covalent bonding is associated with a network forming behavior, whilst an ionic bonding is related to glass modifier properties [12]. Recently, PbO glasses have been restricted in different industries due to it is hazardous to human, animal or environment [13]. On the other hand, the appearance of the germanate anomaly in lead germanate glasses remains an open question. Some researchers conclude that a change of the Ge-O distance from 1.872 to 1.902 Å and an increase in the coordination number occurred with increasing PbO content in the glassy network. The ratio $[GeO_4]$ to $[GeO_6]$ structural units was estimated at 3:1 in the high PbO content

* Corresponding author: khamirul@upm.edu.my

and the coordination number was 4.77 [14]. Therefore, the existence of the germanate anomaly existence in lead–germanate glasses, again stressing that the effect is less pronounced in the glasses with oxides of alkali metals [15, 16].

Heavy metal oxides such as bismuth oxide (Bi_2O_3) can be inserted into germanate glasses. These glasses possess high refractive index, and exhibit large optical basicity, large optical susceptibility values and large polarizability [17-20]. In this setting, Bi_2O_3 has been a convenient replacement of PbO in glass system because it has important properties like low melting. Binary PbO-GeO_2 glass has been reported to show interesting structural and elastic properties. Studies on effect of PbO replacement by Bi_2O_3 on shielding properties of GeO_2 glass system are very limited. The objectives of this work are to calculate shielding properties of BPG glasses.

2. Theory

The mass attenuation coefficient (μ/ρ) values of the glasses materials were calculated by using mixture rule ($(\mu/\rho)_{glass} = \sum_i^n w_i (\mu/\rho)_i$) where w_i is the proportion by weight and $(\mu/\rho)_i$ is mass attenuation coefficient of the i[th] element by using WinXcom [21]. The μ/ρ of the glasses were determined by the transmission method according to Lambert-Beer's law ($I = I_0 e^{-\mu_m t}$), where I_0 and I are the incident and attenuated photon intensity, respectively, μ_m ($cm^2.g^{-1}$) is the linear attenuation coefficient and *t* is the mass thickness of the slab [22]. The thickness of the slab is optimized according to the energy of the incident beam, to avoid that all the photons are absorbed in the slab or traverse the slab without interacting. The primary photons emerging unperturbed from the slab are counted. The energy range of incident photons varied between 1 keV and 100 GeV. The mean free path (MFP) is reciprocal of linear attenuation coefficient. The linear attenuation coefficient is calculated by multiplication of mass attenuation coefficient and density of the glasses. Half value layer (HVL) is calculated by using linear attenuation coefficient using formula HVL(cm)=0.693/μ [23, 24].

The macroscopic effective removal cross section for fast neutrons ($\sum_R$) is the probability of a neutron undergoing certain reaction per unit length of moving through the shielding material. The $\sum_R$ values for the present glasses can be calculated by using the relation [22]:($\sum_R = \sum_i^n W_i (\sum_R/\rho)_i$),where $\sum_{R/\rho}$ (cm^2/g) and W_i represent the mass removal cross-section of the *i*th constituent and the partial density (g/cm^3) respectively.

3. Results and discussion

3.1 Mass attenuation coefficient (μ/ρ)

Glass composition, density of the ternary BPG glasses of the ternary form x(Bi_2O_3)40-x(PbO)60(GeO_2) are given in Table 1. The variation in the mass attenuation coefficient values of the lead bismuth germinate glasses (BPG) containing different concentration of Bi_2O_3 with incident photon energy is shown in the Fig. 1. As shown in Figure 1, the μ/ρ decrease rapidly from 3.37×10^3 to $9.81\times10^{-2}cm^2/g$, 3.59×10^3 to $1.01\times10^{-1}cm^2/g$, 3.75×10^3 to $1.03\times10^{-1}cm^2/g$, 3.87×10^3 to $1.04\times10^{-1}cm^2/g$ and 4.68×10^3 to $1.05\times10^{-1}cm^2/g$ for 0, 10, 20, 30 and 40 mol% Bi_2O_3 respectively, as the photon energy increase up to 0.6MeV. Also, in this energy range, the K-, L- and M-absorption edges have been observed of Ge, Pb and Bi due to the photoelectric effect. This behavior of μ/ρ with photon energy may be attributed to the photoelectric absorption cross-section which is inversely proportional to photon energy $E^{-3.5}$ [25]. In the photon energy range $0.8 < E < 10$ MeV, the μ/ρ values of BPG glasses decrease slowly, from 0.0759 to 0.0396 , 0.0772 to 0.0406, 0.0781 to 0.0414 , 0.0788 to 0.04120 and 0.0794 to 0.0424 cm^2/g for 0, 10, 20, 30 and 40 mol% Bi_2O_3 respectively. It worth noting that in this energy range, the difference between the values of μ/ρ becomes nearly zero. This can be explained on the basis of the dominance of the Compton

scattering, in which, the Compton scattering cross-section is inversely proportional to the incident photons energy (E^{-1}) and linearly change with atomic number Z. Furthermore, it can be seen from Fig.1 that beyond 11 MeV, the values of μ/ρ increase slowly and become constant above 600 MeV. This may be attributed to the pair production process in which and its cross-section depends on atomic number as (Z^2) is predominant mechanism. Finally, from Fig. 1, It is evident that the values of μ/ρ of the BPG glasses increase with increase in the concentration of Bi_2O_3, therefore the values of μ/ρ of BPG glass sample containing 40% mol Bi_2O_3 are largest.

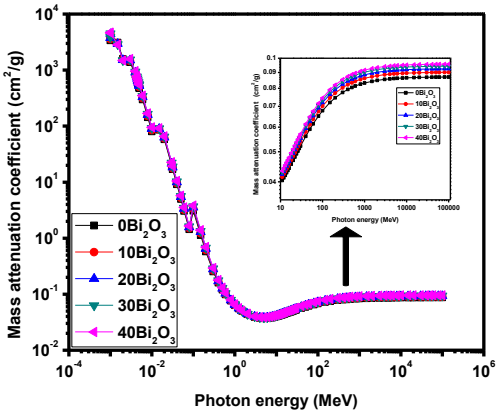

Fig. 1. Variation of mass attenuation coefficient (μ/ρ) of BPG glasses as a function of incident photon energy for total photon interaction from1 keV to 100 GeV

Table 1. Glass composition and density of the ternary BPG glasses

Samples	Glass Composition (mol%)			Density
	Bi_2O_3	PbO	GeO_2	(gcm^{-3})
BPG1	0	40	60	5.90
BPG2	10	30	60	5.91
BPG3	20	20	60	5.99
BPG4	30	10	60	6.01
BPG5	40	0	60	6.05

3.2 Mean free path

The MFP represents the mean distance traveled by moving particles between two successive collisions with other particles. Figure 2 presents the variation of MFP values with incident photon energy in the range 1 keV-100 GeV. It can be seen from Fig.2 that the MFP values for energy less than 0.1 MeV are almost photon energy and composition samples independent. Also, the values of MFP are very small (fraction of cm) in this energy region. With further increase of photon energy, the values of MFP increase rapidly with increasing photon energy and reach maximum value at about 10 MeV. Thereafter, the MFP values decrease and then become almost constant (at 3000 MeV). For the significant nuclear radiation protection of mixture or composite materials, lower values of MFP are desired. From Figure 2 it is clear that the MFP values decrease with an increase in the concentration of Bi_2O_3, which indicates that for an improved shielding effectiveness of BPG glasses, a large Bi_2O_3 content would be required.

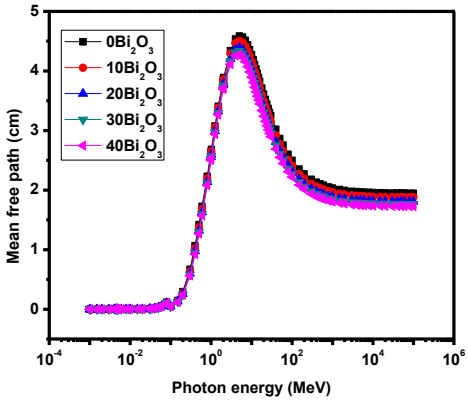

Fig. 2. Variation of mean free path (MFP) of BPG glasses as a function of incident photon energy for total photon interaction from1 keV to 100 GeV

3.3 Half value layer

Fig. 3 shows the half value layers HVL of BPG glasses compared with some shielding glasses which are available in the literature; x=20 [26],GS7 [27], S7 [28] and 70BaO:30SiO2 [29] glasses. The BPG glasses have lower values of mfp than the aforementioned glasses from 100 keV to 100 GeV. In the light of these results, we can conclude that BPG glasses with suitable Bi_2O_3 content have shielding properties that is better than some standard glass systems.

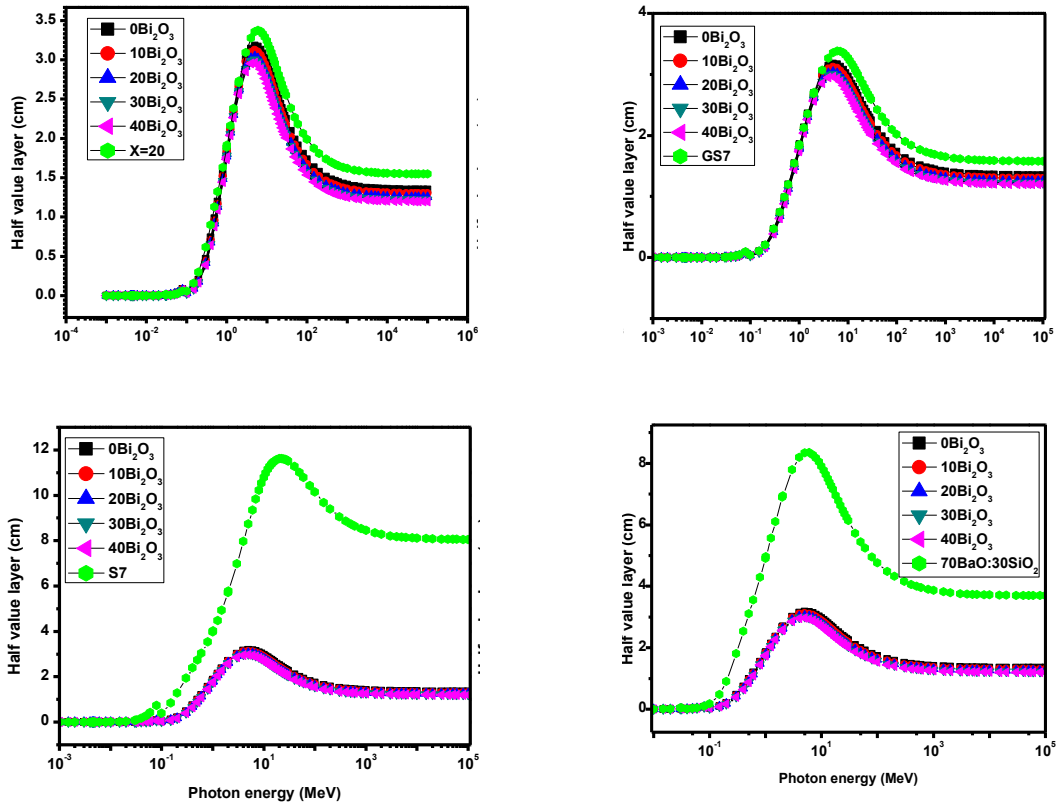

Fig. 3. Half value layer of BPG glasses and different types of glass systems in the energy region of 1 keV–100 GeV

3.4 The macroscopic effective removal cross section for fast Neutrons ($\sum_R$)

The effective removal cross-sections for fast neutron $\sum_R$ of BPG glasses were found as 0.1167 cm^{-1}, 0.1174 cm^{-1}, 0.1195 cm^{-1}, 0.1204 cm^{-1} and 0.1218 cm^{-1} for 0, 10, 20, 30 and 40 mol% Bi_2O_3 respectively. It was observed that the Σ_R values of the investigated glasses were lesser than ordinary concrete (0.0937 cm^{-1}) . In addition, it was found that the values of $\sum_R$ values of the BPG glasses were greater than $80TeO_2$-$20ZnO$, $80TeO_2$-$20K_2O$ [22], $70Bi_2O_3$: $30SiO_2$ and $70Bi_2O_3$: $30B_2O_3$ glasses [29] as illustrated in Fig, 4.

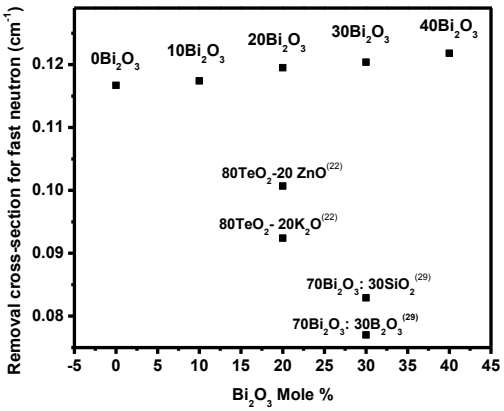

Fig. 4. Removal cross section for fast neutron of BPG glasses and different types of glass systems

4. Conclusions

In this work, the gamma-ray shielding performance of the investigated glass systems was studied using mass attenuation coefficients, mean free path and half value layer. The glass with largest Bi_2O_3 concentration is superior gamma shielding. The investigation would be very useful for shielding applications in nuclear technologies.

Acknowledgments

The researchers gratefully acknowledge the financial support for this study from the Malaysian Ministry of Higher Education (MOHE) and Universiti Putra Malaysia through the Fundamental Research Grant Scheme (FRGS) and *Inisiatif Putra Berkumpulan* (IPB) research grant.

References

[1] Z. Pan, S. H. Morgan, A. Loper, V. King, B. H. Long, W. E. Collins, Journal of Applied Physics **77**(9), 4688 (1995).
[2] Z. Pan, S. H. Morgan, Journal of Non-Crystalline Solids, **210**(2), 130 (1997).
[3] S. S. Bayya, G. D. Chin, J. S. Sanghera, I. D. Aggarwal, Optics Express **14**(24), 11687 (2006).
[4] V. V. Dvoyrin, V. M. Mashinsky, L. I. Bulatov, I. A. Bufetov, A. V. Shubin, M. A. Melkumov, E. F. Kustov, E.M. Dianov, A.A. Umnikov, V.F. Khopin, M. V. Yashkov, Optics letters **31**(20), 2966 (2006).
[5] J.Wu, Z. Yao, J. Zong, S. Jiang, Optics letters **32**(6), 638 (2007).
[6] S. Mailis, C. Riziotis, J. Wang, E. Taylor, A. A. Anderson, S. J. Barrington, H.N. Rutt, R.W. Eason, N. A. Vainos, C. Grivas, Optical Materials **12**(1), 27 (1999).
[7] T. Som, B. Karmakar, Optical Materials **31**(4), 609 (2009).

[8] M. Wachtler, A. Speghini, K. Gatterer, H. P. Fritzer, D. Ajo, M. Bettinelli, Journal of the American Ceramic Society **81**(8), 2045 (1998).
[9] M. Hamezan, H. A. A. Sidek, A. W. Zaidan, K. Kaida, A. T. Zainal, J. Appl. Sci. **6**(4), 943 (2006).
[10] K. A. Matori, M. H. M. Zaid, H. A. A. Sidek, M. K. Halimah, Z. A. Wahab, Journal of Non-Crystalline Solids **361**, 78 (2013).
[11] L. Żur, J. Janek, M. Sołtys, T. Goryczka, J. Pisarska, W. A. Pisarski, Journal of Non-Crystalline Solids **431**, 145 (2016).
[12] R. Ciceo-Lucacel, I. Ardelean, Journal of Non-Crystalline Solids **353**(18), 2020 (2007).
[13] P. Y. Shih, T. S. Chin, Journal of Materials Science Letters **20**(19), 1811 (2001).
[14] M. Rada, N. Aldea, Z. H. Wu, Z. Jing, S. Rada, E. Culea, S. Macavei, R. Balan, R.C. Suciu, R. V. Erhan, V. Bodnarchuk, Journal of Non-Crystalline Solids **437**, 10 (2016).
[15] A. Witkowska, B. Sikora, K. Trzebiatowski, J. Rybicki, Journal of Non-Crystalline Solids **352**(40), 4356 (2006).
[16] S. Rada, E. Culea, M. Rada, Journal of Non-Crystalline Solids **356**(25), 1277 (2010).
[17] P. Pascuta, E. Culea, Materials Letters, **62**(25), 4127 (2008).
[18] G. Zhao, Y. Tian, H. Fan, J. Zhang, L. Hu, Chinese Optics Letters **10**(9), 091601 (2012).
[19] M. Rada, L. Rus, S. Rada, E. Culea, T. Rusu, Spectrochimica Acta Part A: Molecular and Biomolecular Spectroscopy **132**, 533 (2014).
[20] F. Cabello, S. Sanchez-Cortes, M. J. de Castro, Journal of Non-Crystalline Solids **445**, 110. (2016).
[21] L. Gerward, N. Guilbert, K. B. Jensen, H. Levring, Radiation Physics and chemistry **71**, 653 (2004).
[22] M. I. Sayyed, Canadian journal of physics **94**, 1133 (2016).
[23] M. I. Sayyed, H. Elhouichet, Radiation Physics and Chemistry **130**, 335 (2017).
[24] M. I. Sayyed, Journal of Alloys and Compounds **695**, 3191 (2017).
[25] J. H. Hubbell, Phys. Med. Biol. **44**, R1. (1999).
[26] M. I. Sayyed, Journal of Alloys and Compounds **688,** 111 (2016).
[27] K. A. Matori, M.I. Sayyed, H.A.A. Sidek M.H.M. Zaid, V.P. Singh, Journal of Non-Crystalline Solids **457**, 97 (2017).
[28] V. P. Singh, N.M. Badiger, Glass Phys. Chem. **41**, 276 (2015).
[29] V. P. Singh, N.M. Badiger, J. Kaewkhao, J. Non-Cryst. Solids **404**, 167 (2014).